European Journal of Pharmaceutics and Biopharmaceutics 80 (2012) 194–202

Contents lists available at SciVerse ScienceDirect

European Journal of Pharmaceutics and Biopharmaceutics

journal homepage: www.elsevier.com/locate/ejpb

Research paper

Preparation and solid-state characterization of ball milled saquinavir mesylate for solubility enhancement

Michael Lee Branham [a,*], Thomas Moyo [b], Thirumala Govender [a]

[a] School of Pharmacy and Pharmacology, University of KwaZulu-Natal, Durban, South Africa
[b] School of Physics, University of KwaZulu-Natal, Durban, South Africa

ARTICLE INFO

Article history:
Received 3 May 2011
Accepted in revised form 19 August 2011
Available online 30 August 2011

Keywords:
Saquinavir
Solubility enhancement
Ball milling
Solid-state characterization
Nanosizing
Drug delivery

ABSTRACT

Saquinavir is an anti-retroviral drug with very low oral bioavailability (e.g. 0.7–4.0%) due to its affinity toward efflux transporters (P-gp) and metabolic enzymes (CYP3A4). The aim of this study was to characterize the effects of high-energy ball milling on saquinavir solid-state characteristics and aqueous solubility for the design of effective buccal drug delivery systems. The solubility of saquinavir mesylate was evaluated in simulated saliva before and after milling for 1, 3, 15, 30, 50, and 60 h. To elucidate changes in crystallinity and long-range structure in the drug, analyses of the milled powders were performed using XRD, ATR-IR, DSC/TGA, BET surface area, EDX and SEM. In addition, the effects of milling time on saquinavir solubility were statistically correlated using repeated measures ANOVA. Results of this study indicate that the milling of saquinavir mesylate produces nanoporous particles with unique surface structures, thermal properties, and increased aqueous solubility. Optimal milling time occurred at 3 h and corresponded to a 9-fold solubility enhancement in simulated saliva. Thermal analysis revealed only a slight decrease in melting point (T_m) from 242 °C to 236 °C after 60 h milling. XRD diffractograms indicate a gradual crystalline-to-amorphous transition with some residual crystallinity remaining after 60 h milling time. Unstable polymorphic structures appeared between 15 and 30 h which were converted to more stable isomorphs at 60 h. Aggregate formation also seems to occur after 15 h but no metal contamination of the drug was observed during the milling process as determined by EDX analysis. In conclusion, high-energy ball milling may be a method of choice for improving the solubility of saquinavir and facilitating novel drug formulations design.

1. Introduction

The discovery of HIV protease inhibitors has introduced new and effective first-line therapies for HIV/AIDS. However, many of these drugs still suffer from poor bioavailability due to low aqueous solubility and/or membrane permeability [1,2]. These are structurally related "peptidomimetic" compounds, with higher molecular weights than conventional drugs and relatively high lipophilic character as demonstrated by their octanol–water partition coefficients (i.e., Log*P*). Also common is their characteristic pH-dependent solubility [2], each being poorly soluble at physiological pH (>6.0) but soluble at low pH (<5.0).

An archetypal protease inhibitor, saquinavir, has molecular weight (767.0 g/mol), Log*P* (4.1), and permeability coefficient (1.5×10^{-6} cm/s) typical of other drugs in its class. Its aqueous solubility has been reported (73 mg/L at pH = 6.5, 36 mg/L at pH = 7.4) along with at least two ionization constants (p*K*a 7.0 and 5.5) but conflicting reports can still be found in the literature [3–6]. As a result, the oral bioavailability of saquinavir is reported to be very low (0.7–4.0%), depending upon the dosage form considered. In addition to its poor solubility, saquinavir is metabolized by both human hepatic and small intestinal microsomes [7,8]; therefore, pre-systemic elimination of the drug plays a critical role in its low bioavailability. Molecules of this type provide a number of challenges to drug delivery scientists, particularly when the oral route of administration is being developed. A large number of novel approaches for enhancing low aqueous solubility of drugs have been proposed. These strategies include methods to reduce particle size and increased surface area [9], the use of alternative salt forms [10], solubilization of the drug in co-solvents [11] or micellar solutions [12], complexation with cyclodextrins [13] or the use of lipid-based vehicles for the delivery of lipophilic drugs [14]. Although some of these techniques have been effective at enhancing oral bioavailability for specific compounds, success is usually marginal and highly dependent on the physicochemical properties of the drug. Antiretroviral drug delivery via the buccal route would be an effective means to increase their systemic bioavailability, but only if their solubility in oral fluids could be improved. We

* Corresponding author. School of Pharmacy and Pharmacology, University of KwaZulu-Natal, Durban, South Africa. Tel.: +27 0312607358; fax: +27 0312607792.
E-mail address: Branham@ukzn.ac.za (M.L. Branham).

0939-6411/$ - see front matter © 2011 Elsevier B.V. All rights reserved.
doi:10.1016/j.ejpb.2011.08.005

therefore investigated the effects of high-energy ball milling on saquinavir aqueous solubility and solid-state properties.

The solid-state characteristics, particle size, and crystallinity are very important considerations because of their influence on drug stability, flowability, and dissolution rate. Here, the effects of milling on particle size, pore structure, and crystal morphology were first observed with the drug digoxin [15,16]. Later reports on improved solubility [16] and bioavailability [17] of poorly absorbed drugs after milling lead to a rapid increase in the application of micronization [18] and nanosizing [19,20] by commercial drug developers.

Currently, micronization via air-jet mill is a common industrial practice to reduce drug particle size because it can be operated using conventional milling equipment. Reductions in particle diameter to the range 2–5 μm are typically achieved, but this may not provide sufficient increases in aqueous solubility or bioavailability for some drugs (e.g., lipophilic protease inhibitors). In these cases, advanced milling technologies such as high-pressure homogenization [21,22], "wet-milling" technology [22,23], milling in cryogenic-fluids [24], and the supercritical fluid-processing [25] are being investigated. These technologies are capable of reductions in particle size to 100–250 nm, providing a considerable increase in surface area and solubility. In addition to particle size reduction, the formation of amorphous solids or solid dispersions has been shown to enhance solubility as well [26]. Pharmaceuticals are typically manufactured in a stable crystalline form because the amorphous form tends to convert to the crystalline form due to its thermodynamic instability. However, despite this clear disadvantage, the amorphous state has attracted considerable interest in recent years [27,28].

Saquinavir exhibits extended pseudo-polymorphism, as described by the manufacturer. Amorphous saquinavir is prepared from a crystalline ethyl ester solvate, which may collapse upon evaporation of the solvent, leading to a disordered structure of the drug. Compared to many other pharmaceutical compounds that are highly unstable in the amorphous form [29,30], the free base of saquinavir is reported to remain amorphous even at stressed stability conditions [31]. In contrast, the mesylate salt of saquinavir contains substantial amounts of trace crystallinity, which may be an important factor in its low aqueous solubility. Thus, the limited solubility of saquinavir may be overcome using ball milling techniques and conditions to prepare solid dispersions with optimal surface area and porosity.

In this study, solid dispersions of saquinavir mesylate (SQVM) were prepared by ball milling from 1 to 60 h in order to enhance its aqueous solubility and increase surface area. High-energy ball milling has the advantage of generating an amorphous system while simultaneously promoting the formation of crystalline domains of reduced particle size. Saquinavir solubility in aqueous buffers were then determined and correlated with the duration of the milling time. In addition, physical characterization and repeated measures ANOVA were used to compare the solid dispersions before and after milling to obtain information about potential differences in the molecular structure, crystallinity, surface area and porosity, density, and phase transition temperatures. Potential applications of pre-milled anti-retroviral drugs in the development of buccal drug delivery systems and planned future investigations are also discussed.

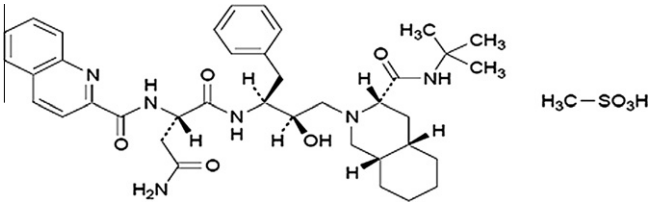

Fig. 1. Saquinavir mesylate. CAS Reg. No. 149845-06-7.

2. Materials and methods

2.1. Materials

Saquinavir mesylate (Fig. 1) was kindly donated by Hoffmann-La Roche Ltd. (Basel, Switzerland) and analyzed as received before and after milling for 1–60 h. All other reagents used (NaCl, KCl, $NaHCO_3$, Na_2HPO_4, NaH_2PO_4, KH_2PO_4, NaOH, MeOH, and H_3PO_4) were of analytical grade. Purified water used in the solubility studies was produced in the laboratory with a Milli-Q purification system (Millipore Corp., USA).

2.2. Methods

2.2.1. Preparation of nanoporous saquinavir: high-energy ball milling

The ball milling was performed in a high-energy planetary mill (Retsch PM 400) at room temperature under compressed air. Stainless steel milling jars (250 mL) containing an appropriate mass of balls (15 mm) of the same material. One gram of SQVM was milled for 1, 3, 15, 30, 50, and 60 h in each jar with a ball/sample weight ratio of 30:1. The speed of the solar disk was set to 200 rpm.

2.2.2. Solid-state characterization of nanoporous saquinavir mesylate

2.2.2.1. Nuclear magnetic resonance spectroscopy (NMR). ^{1}H NMR and ^{13}C NMR spectra of saquinavir mesylate were obtained using the Brucker Avance-III 500 (11.7 T) instrument operating at 500 MHz (proton frequency) and 125 MHz (carbon frequency). Samples were prepared by dissolution in CD_3OD (99.9%). Chemical shifts were reported in ppm (δ) downfield from tetramethylsilane (TMS) internal reference.

2.2.2.2. Attenuate total reflectance-infrared spectroscopy (ATR-IR). FTIR spectra of all drug products were recorded on an Alpha Platinum FTIR spectrophotometer (Bruker, Bryanston, ZA). The instrument was configured with a Pike ATR sample cell including a diamond crystal with a scanning depth up to 2 μm. Sample powders were applied to the surface of the crystal then locked in place with a "clutch-type" lever before measuring transmittance. Each of the spectra was collected in the range 4000–400 cm^{-1} at 2 cm^{-1} resolution.

2.2.2.3. Differential scanning calorimetry/thermogravimetric (DSC/TGA). DSC/TGA thermograms of milled and un-milled drug samples were obtained using a TA Instruments SDT-Q600 thermal analyzer (AMS Laboratory Technologies Ltd., Cape Town, South Africa) equipped with a computerized thermal data analyzer. Drug samples were weighed (5–10 mg) in flat-bottomed aluminum pans and heated from 30 to 350 °C at 5 °C/min under a nitrogen purge gas flowing at a rate of 5 mL/min. Single point melting temperatures of the samples before and after milling were also determined manually using a Stuart® melting point apparatus (Sigma–Aldrich, St. Louis, MO).

2.2.2.4. X-ray powder diffraction (XRD). X-ray powder diffraction patterns were recorded using a monochromatic beam of Co Kα radiation (λ = 1.7903 Å) on a Phillips X Pert diffractometer (PANalytical B.V. Twentepoort, Netherlands). The positions of the X-ray tube and detector were checked by using zero point definition of the 2θ scale. The measurements were performed in symmetrical reflection mode at 40 kV and 40 mA. The powder samples were scanned in the angular range of 5–80° 2θ with a step size of 0.01° and a count time of 1 s per step.

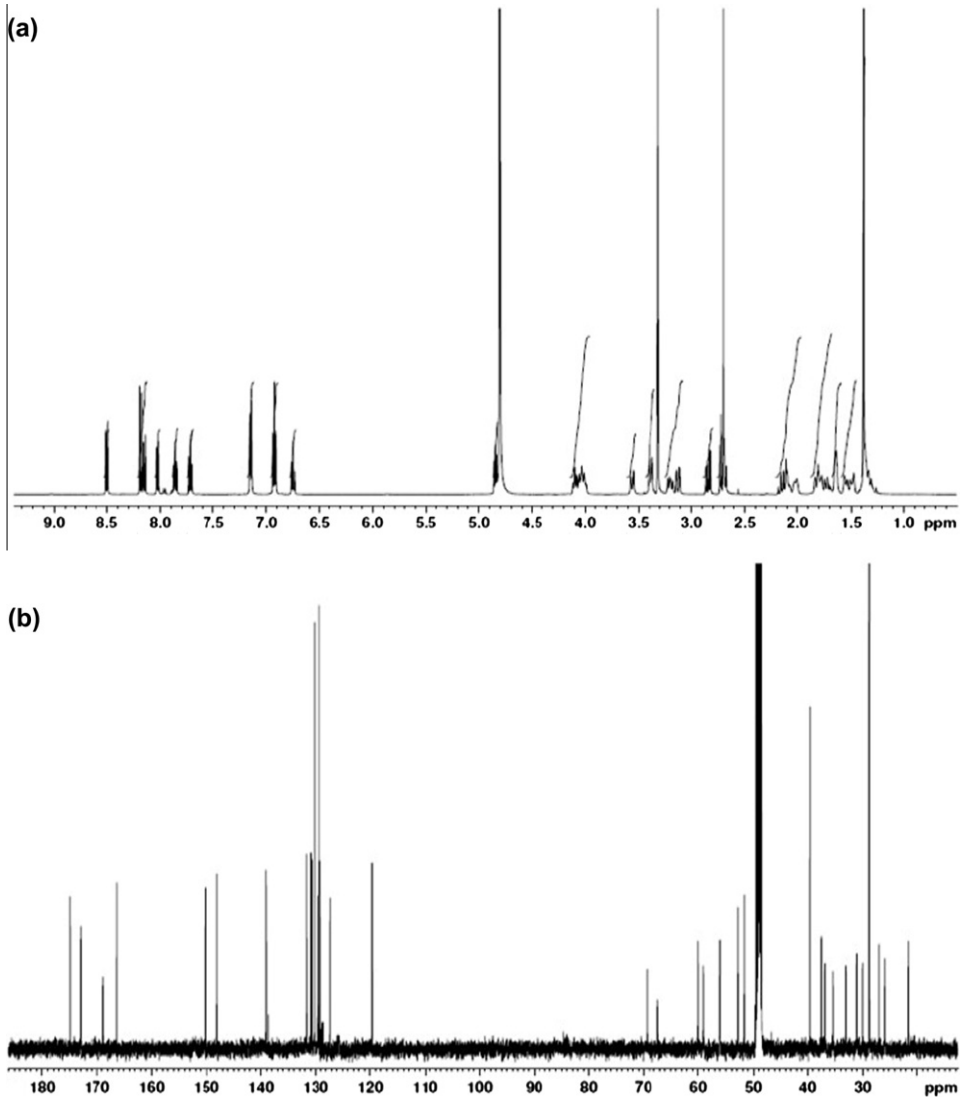

Fig. 2. NMR spectra: (a) ^{1}H NMR spectra and (b) ^{13}C NMR spectra.

2.2.2.5. BET surface area and porosity. Surface properties including BET surface area (m^2/g), total pore volume (μL/g), and mean pore diameter (nm) were determined from N_2 adsorption isotherms determined at −195.8 °C with a Micrometrics Tristar II 3020 (Micromeritics Instrument Corp. Norcross, GA, USA). Specific surface areas were calculated with the BET equation [34] and pore size distribution with the BJH method [35]. The total pore volume (surface and bulk) was taken from the adsorption branch of the isotherm at $P/P0 = 0.98$, assuming complete pore saturation. Particle size estimates were calculated for each of the samples after milling from BET surface area and density using the spherical approximation method (particle diameter = 6/(surface area)/(density).

2.2.2.6. Field Emissions Scanning Electron Microscopy (FESEM). Saquinavir pellets were produced in an evacuated 13 mm die chamber using a Air-EZ™ Press (International Crystal Laboratories, Garfield, NJ) at 2 tons for approximately 2 min. Density of the milled and un-milled pellets was determined manually from their mass and dimensions measured with a micrometer. Scanning electron micrographs of milled and un-milled saquinavir mesylate pellets were obtained using a high-resolution field-emission scanning electron microscope, JEOL-JSM 7500F (JEOL Ltd., Herts, England) operating at an accelerating voltage of 1 kV. The samples were fixed onto brass stubs using double-sided adhesive tape then coated with a thin carbon layer in a sputter coating unit (VG Microtech, UK).

2.2.2.7. Aqueous solubility assessments. The aqueous solubility of milled and un-milled drug was determined in simulated saliva with the aim to mimic conditions present on the surface of the buccal mucosa [32]. Simulated saliva was prepared with 2.38 g Na_2HPO_4, 0.19 g KH_2PO_4, 8.00 g NaCl in 1000 mL of distilled water with the pH value adjusted to 6.8 with orthophosphoric acid [33]. Excess amounts of drug was placed in 100 mL shake flask then mixed at 25 °C for 72 h. This solution was then filtered through 0.22 μm syringe filter before concentration measurement via UV spectrophotometric absorbance at 239 and 210 nm.

2.2.3. Statistical data analysis

Repeated measures analysis of variance was used to analyze the relationship between solubility and drug milling time. A two-factor design (i.e., absorbance wavelength 210 or 239 nm) with repeated measures at different milling times (1, 3, 15, 30, 50, and 60 h) was applied followed by Tukey's multiple comparisons ($p < 0.05$) using MedCalc® v.12. (MedCalc Software bvba., Belgium). A clustered multiple variables graph was plotted to show trends in the data.

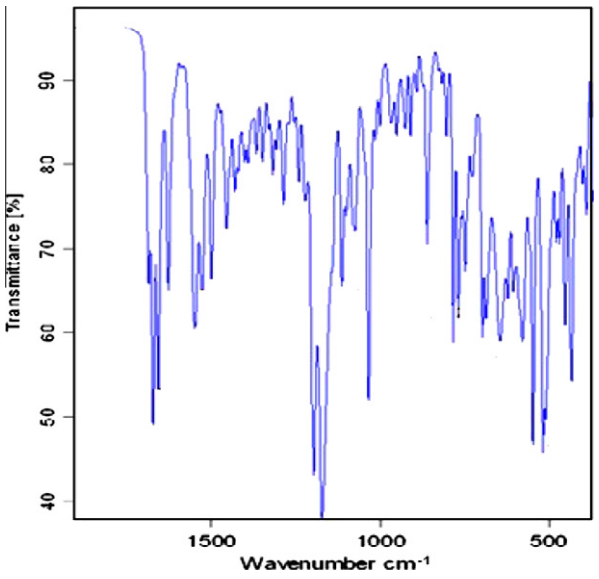

Fig. 3. Saquinavir mesylate ATR-IR spectra. (For interpretation of the references to color in this figure legend, the reader is referred to the web version of this article.)

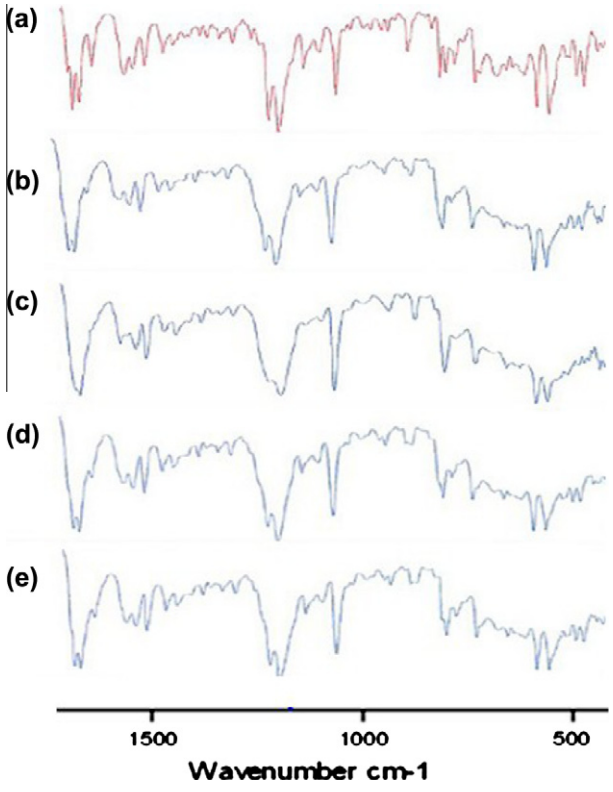

Fig. 4. Effects of milling on saquinavir mesylate IR spectra. (For interpretation of the references to color in this figure legend, the reader is referred to the web version of this article.)

3. Results

3.1. Effects of milling on saquinavir molecular structure and physicochemical properties

3.1.1. ^{1}H NMR and ^{13}C NMR

Fig. 2a and b exhibit the proton and carbon NMR spectra of saquinavir, respectively. Functional groups for aromatic hydrogens corresponding to chemical shifts at δ = 6.7 ppm, 6.9 ppm, 7.1 ppm, 7.75 ppm, 7.9 ppm, 8.05 ppm, 8.1 ppm, 8.14 ppm, and 8.5 ppm agree with previous studies [4,43]. The dominant peaks were at 1.35 ppm for the 9 nine t-butyl hydrogens and at 4.7 ppm represented the signal due to H_2O [43]. The presence of the unique hydroxyl group (C-26) was unambiguously confirmed by chemical shifts at δ_H = 3.58 and δ_C = 69.4 ppm. Similarly, signals for the mesylate salt were confirmed at δ_H = 4.1 and δ_C = 36.4 ppm.

3.1.2. ATR-IR

The FTIR spectra of milled and un-milled saquinavir are presented in Fig. 3. The un-milled drug exhibited an amide absorption band in the range of 1680–1630 cm^{-1}. The strong peak (#9) at 1672 cm^{-1} confirms the presence of multiple secondary amides in the sample. The amide carbonyl (amide band I) stretching band occurred as a multiplet, suggesting the simultaneous presence of different stretching modes. The first peak (#8) at 1685 cm^{-1} corresponds to intermolecular hydrogen bonded carbonyl groups, while peaks (#10 and 11) at 1657 and 1627 cm^{-1} maybe explained by the presence of free carbonyl groups in the crystal lattice of SQVM. These peaks are also representative of milling induced transitions in long-range structure that occurred between 3 and 15 h milling and again between 15 and 30 h. The bands (#12, 13, and 14) centered at 1528 cm^{-1} representing characteristic amide II vibrations do not seem affected by milling.

In addition, sulfonyl absorption band (#16, 17, and 18) at 1197, 1174, and 1115 cm^{-1} corresponding to stretching vibrations of hydrogen bonded S–O groups is representative of the mesylate salt form. This absorption pattern was affected by milling time and suggests a polymorphic conversion starting at 15 h. Fig. 4 shows that the each of the spectra is practically superimposable except for the changes mentioned above. These observations indicate that the ball milling procedure has little effect on molecular structure but may have a substantial effect on hydrogen-bonding and crystallinity of the drug.

3.1.3. Thermal analysis

Fig. 5 presents the DSC/TGA thermograms of saquinavir mesylate. Each curve (i.e., a, b, and c) shows an endotherm at about 39 °C that may be due to the evaporation of volatile materials and moisture followed by transient cooling in the sample. The largest weight loss (6.7%) due to dehydration was observed in the 60 h milled sample, most likely due to its greater moisture content. A glass transition may be embedded with the dehydration endotherm as reported in other thermal analyses of amorphous saquinavir at that temperature [39]. The endotherms at 242 °C correspond to the melting point of un-milled saquinavir mesylate and after milling for 3 h (238 °C) and 60 h (236 °C). There were also exothermic peaks near 180, 275, and 310 °C that appear at 60 h milling which may be due to additional cooling, cross-linking, oxidation, or polymorph conversion of the drug. SQVM decomposition begins at about 262 °C, which is slightly lower for the 60 h milled as indicted by the slope of TGA thermogram. The major weight loss transition occurs between 250 and 300 °C. This weight loss step in TGA coincides with the exothermic decomposition peak in the DSC curve.

3.2. Effects of milling on saquinavir long-range structure and crystallinity

3.2.1. X-ray powder diffraction (XRD)

The X-ray diffraction patterns of un-milled and milled saquinavir mesylate are shown in Fig. 6. In the X-ray diffraction pattern of the un-milled drug (Fig. 6a), several peaks are observed at an angular positions 15–30°, which declines and broadens with increased milling time, and this resulted in a characteristic amorphous halo observed at 30 h. Diffractograms (a, b, and e) illustrate corresponding peaks at 44.4°, 52°, and 78°, suggesting presence of isomorphic

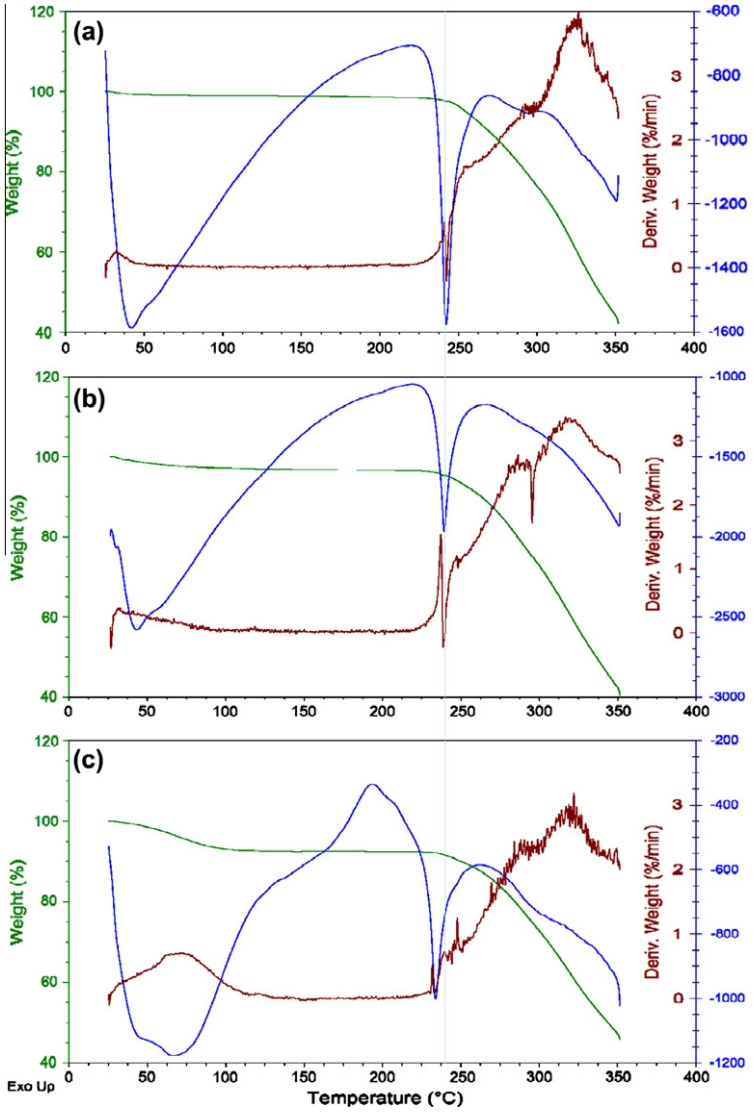

Fig. 5. Thermal analysis of saquinavir mesylate. DSC/TGA thermograms for saquinavir are presented at (a) 0, (b) 3, and (c) 60 h ball milling. (For interpretation of the references to color in this figure legend, the reader is referred to the web version of this article.)

structures at 3 and 60 h milling to the starting material. This implies that the three-dimensional arrangement of the drug molecules has a common structural motif (conformation and packing) or that included solvent molecules occupy common crystallographic sites. Ball milling of the drug, however, causes these structures to collapse, resulting in corresponding amorphous material. In contrast, changes in the diffraction patterns at 15 and 30 h resulted in a substantial shift in these high intensity peaks to positions at 50°, 52°, and 57° (2θ) and returned back after 60 h (Fig. 6c–e). This suggests that in addition to the crystalline/amorphous transition new but unstable polymorphic structures are formed at 15 and 30 h, which undergo conversion if milling continues to 60 h. It has been observed before that when a solvent is lost from a crystalline solvate structure, three-dimensional order of the crystal lattice may be changed, resulting in polymorphous forms that represent a high-energy state relative to the original solvate structure [36–38]. According to this theory, it is therefore likely that some proportion of the original structure remains intact but that structural relaxation occurs with continued milling as reflected in the amorphous halo in positions 15–30° as seen in Fig. 6c and d. Therefore, it appears that irreversible destruction of the residual crystal lattice is not achieved by mechanical stress through milling of SQVM.

3.2.2. BET surface area and porosity

Experiments were conducted to study the effects of balling milling (1, 3, 15, 30, and 60 h) on saquinavir surface area and porosity. BET surface area plots and the relationships between pore structure, milling time, and solubility are illustrated in Fig. 7. The results show the drug with higher BET surface area, and total pore volume after milling up to 3 h, but lowered values at 15 h in crystal morphology and potential aggregate formations. Various types of pores may be formed (e.g., closed pores, blind pores, and through pore) during mechanical activation of the drug, thus calculation of pore size and diameter may not correlate with milling time as well as the other surface parameters. Results indicated trends in surface area, which were similar to those of pore volume but not of pore diameter. We therefore expect pore structure to extend into the bulk of the material rather than confined to the surface. Nonetheless, the trend is toward smaller diameters and pore size was found to be lowest after 60 h milling. As shown in Table 1, BET surface area, total volume, and pore diameter of milled saquinavir ranges from 14.4 to 1.46 m^2/g, 64.0 to 11.0 μL/g, and 30.6 to 7.7 nm, respectively. Particle size after milling was calculated from density and BET surface area using the spherical approximation method. SQVM particle diameters decreased from approximately 1 μm to 0.35 μm within the 3 h of milling, but increased in diameter

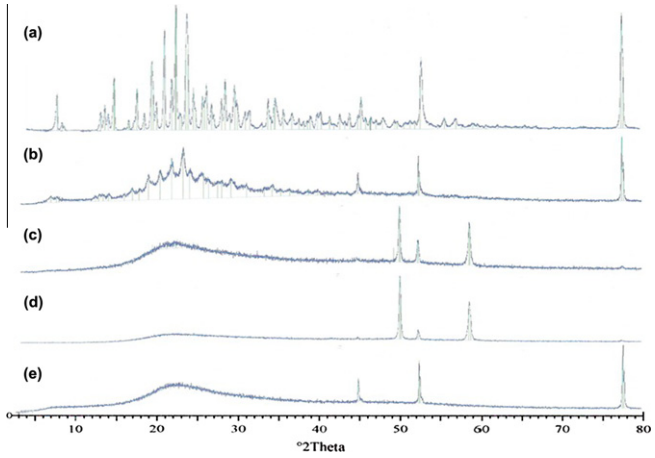

Fig. 6. X-ray Diffractometry: diffractograms are for saquinavir mesylate after milling for (a) 1, (b) 3, (c) 15, (d) 30, and (e) 60 h. (For interpretation of the references to color in this figure legend, the reader is referred to the web version of this article.)

thereafter. From these results, optimal BET surface area and porosity can be achieved at 3 h milling (see Table 1).

3.2.3. Scanning Electron Microscopy (FESEM)

Surface micrographs of saquinavir before and after milling are shown in Fig. 8. Un-milled saquinavir pellets with a relatively roughened surface (Fig. 8a) consists of fused plate-like crystalline structures ranging in size between 2 and 50 μm (Fig. 8d). After 1 and 3 h milling, the surface morphology of the saquinavir pellets changed to a smooth glassy microtexture (Fig. 8b and c) and particles with sizes below 1 μm (Fig. 8e). Plate-like crystalline structures were observed in the bulk of the samples in the submicron range (~300 nm) after 3 h milling (Fig. 8f and Fig. 9). Elemental analysis by electron-dispersive X-ray spectroscopy (EDX) shows (Fig. 10) that no metal contamination of the drug occurs during milling up to 60 h.

3.3. Effect of ball milling on saquinavir aqueous solubility

3.3.1. Aqueous solubility assessments

Table 1 summarizes the experimentally determined solid-state characteristics and solubility of saquinavir mesylate in aqueous buffer. Milling for 3 h resulted in a 9-fold increase in equilibrium solubility of the drug. However, continued milling from 30 to 60 h did not improve solubility further, but instead resulted in small decreases in solubility enhancement. Aqueous solubility versus surface area, pore volume, pore size, and milling time are shown in Fig. 7.

3.3.2. Statistical data analysis

Solubility verses milling time and means clustered by group diagrams are shown in Fig. 11a and b, respectively. Results of a repeat measures ANOVA (Table 2) indicated that milling time has a statistically significant effect on the solubility of saquinavir in aqueous buffers.

4. Discussion

Numerous studies have demonstrated that solid-state structure can have a significant effect on the dissolution rate and bioavailability of poorly soluble drugs [39–42]. Our study confirms some of these previous findings and reports for the first time on the effects of high-energy ball milling on SQVM. We used an extended

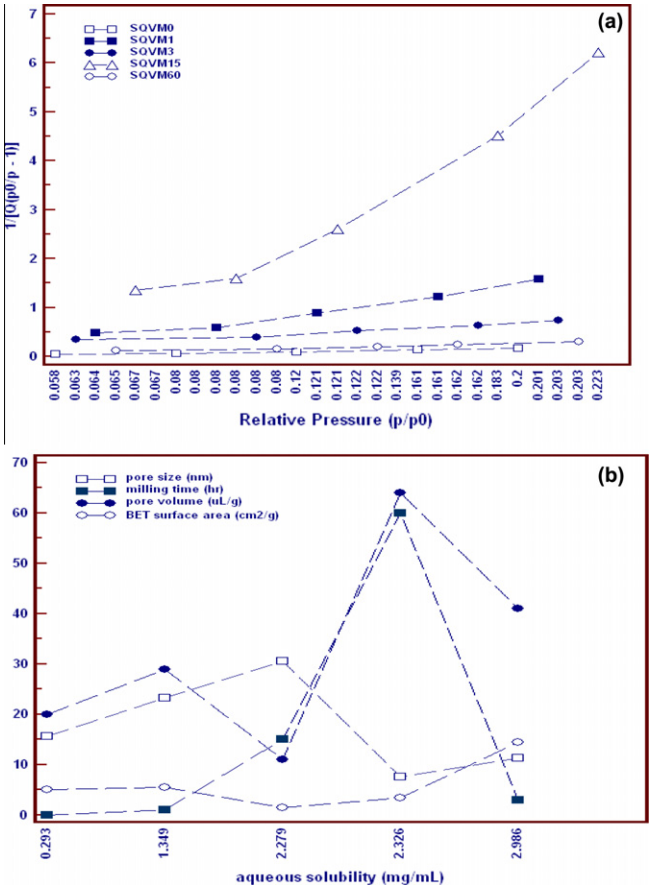

Fig. 7. Surface area and porosity. (a) BET surface area plots are shown that illustrate the inverse linear relationship between relative pressure and total amount adsorbed. In (b), the graph illustrates the relationship between saquinavir solubility and the surface area, pore volume, pore size and milling time. (For interpretation of the references to color in this figure legend, the reader is referred to the web version of this article.)

milling time of 60 h to determine the optimal solubility enhancement possible and the effects of milling on saquinavir crystallinity, surface area, and pores structure. No chemical transformations in molecular structure appear to occur during the milling process. Furthermore, our results compared favorably with other studies of ball milled acetaminophen for this length of time [47].

High-energy ball milling causes rapid increases in surface area and decreases in the primary diameter of drug particles. Conditions in the mill are such that substantial amounts of energy are used to process the drug substance; this can lead to crystalline polymorphic conversions and/or the generation of an amorphous mixture [38]. We refer to these materials as solid dispersions because the transformation between crystalline and amorphous character occurs gradually, and this results in solid mixtures [29,31,39] at the different stages of the milling process.

Recent findings in other drug milling studies propose that grinding simultaneously lowers both the degree of crystallinity and the dehydration temperatures of the ground products. This facilitates the removal of lattice water and results in the formation of drug solids that are very hygroscopic [38,39,41]. The loss of crystalline water upon extensive grinding of hydrate phases is frequently observed, and several researchers report that an amorphous drug at higher energy with respect to its crystalline form requires a lower activation energy for dissolution [27,44,46].

Theories regarding the physicochemical aspects of pharmaceutical milling are also being proposed. The classical description is

Table 1
Saquinavir mesylate solid-state characteristics. Melting points (a) were determined by DSC, particle size (b) were calculated by the spherical approximation method (particle diameter = 6/(surface area)/(density).

Saquinavir mesylate solid-state characteristics							
Ball milling time (h)	0	1	3	15	30	50	60
Solubility (mg/mL)	0.293 ± 0.07	1.349 ± 0.03	2.986 ± 0.02	2.279 ± 0.01	2.979 ± 0.01	2.886 ± 0.06	2.326 ± 0.06
Melting point PC)	[210, [a]242]	n/d	[215, [a]238]	n/d	n/d	n/d	[145, [b]236]
Density (g/mL)	1.149	1.197	1.168	1.210	1.172	n/d	1.195
Particle size[b] (nm)	1030	912	355	3400	n/d	n/d	1500
BET surface area (m^2/g)	5.069 ± 0.17	5.470 ± 0.15	14.43 ± 0.36	1.455 ± 0.092	n/d	n/d	3.365 ± 0.109
Pore volume (μL/g)	20.0	29.0	41.0	11.0	n/d	n/d	64.0
Pore size (nm)	15.59	23.29	11.29	30.58	n/d	n/d	7.66

Table 2
Saquinavir Solubility versus milling time. A repeated measures ANOVA was performed to describe the relationship between ball milling and aqueous solubility measured at two wavelengths. Differences in solubility between samples (i.e., milling) were statistically significant ($p < 0.001$), while the differences in solubility within samples (i.e., absorbance at 239 or 210 nm) were not statistically significant ($p > 0.05$).

Repeated measures ANOVA							
Between-samples factors	($n = 21$)	Test of between-samples effects					
Milling time (h)	*n*	Source of variation	SS	DF	Mean square	*F*	*p*-Value
0	3						
1	3	Group (milling time)	36.39	6	6.064	17189.28	<0.001
3	3						
15	3	Residual	0.00494	16	0.000353		
30	3	Test of between-samples effects					
50	3						
60	3						
Sphericity method	Epsilon	Source of variation	SS	DF	Mean square	*F*	*p*-Value
Greenhouse-Geiser	1.00	Factor	0.000130	1	0.000130	0.37	0.552
Huynh-Feldt	1.00	Group-factor interaction	0.000808	6	0.000135	0.39	0.876
		Residual	0.00489	14	0.000349		

that drug solids obey some form of the Noyes–Whitney model in terms of dissolution velocity in aqueous solutions [40,44]. Here, increases in particle surface area and saturation solubility increase directly with the drug dissolution rate. This notion has been demonstrated by the surface area estimates in our study and the pH-dependence of SQVM saturation solubility in the model has been confirmed by others [6,27].

Researchers [20,37] have rationalized what may be called a "dissolution pressure", using a model analogous to the transfer of molecules in the liquid phase (i.e., droplets) into the gas phase to

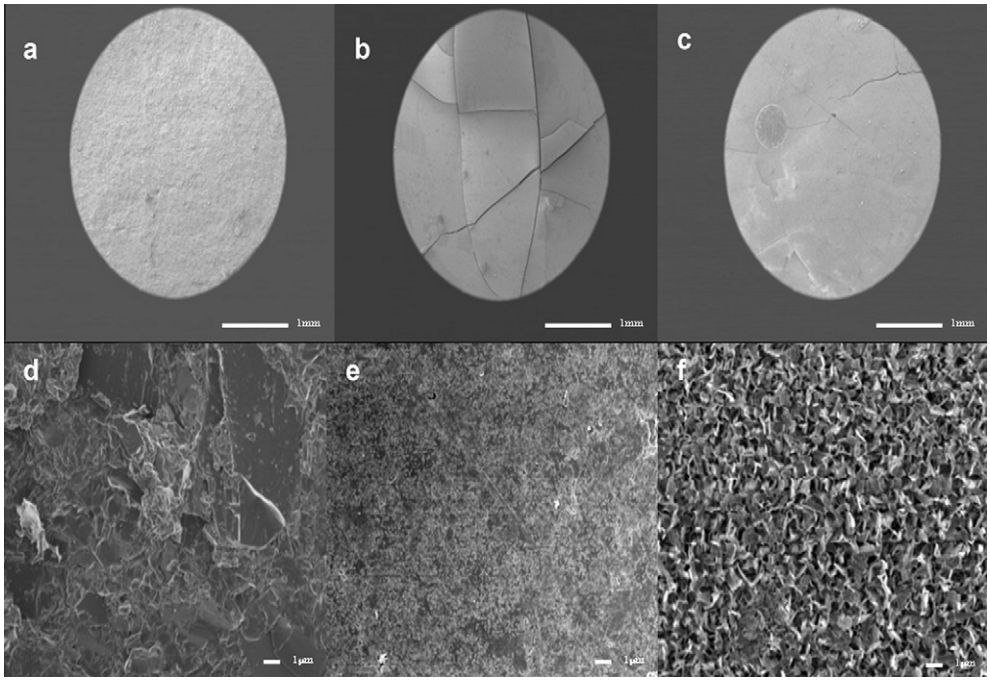

Fig. 8. Scanning electron microscopy. Micrographs for pelletized saquinavir are shown after milling (a) 0, (b) 1, and (c) 3 h. Higher magnification images are shown (d) without milling, (e) after milling for 1 h, and (f) after milling for 3 h.

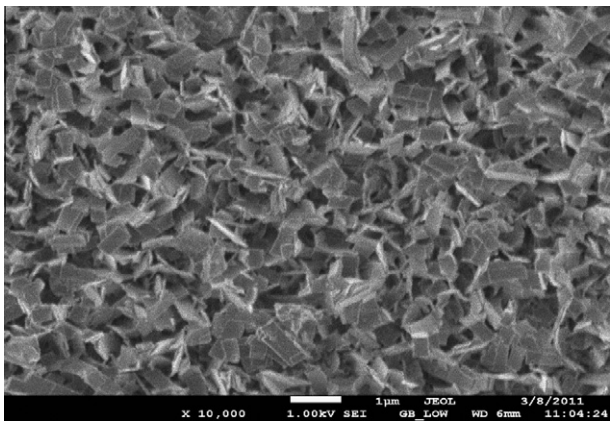

Fig. 9. Nanocrystalline SQVM. Crystal structures (~300 nm) after milling for 3 h.

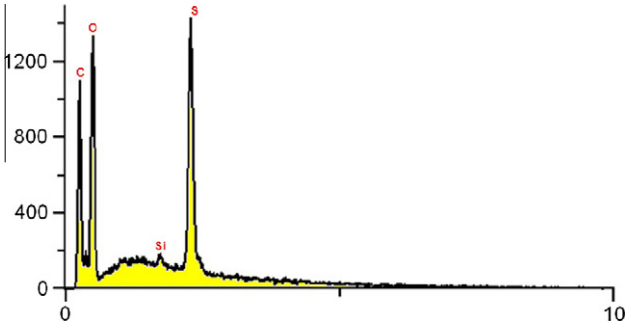

Fig. 10. Energy-dispersive X-ray spectrum. (For interpretation of the references to color in this figure legend, the reader is referred to the web version of this article.)

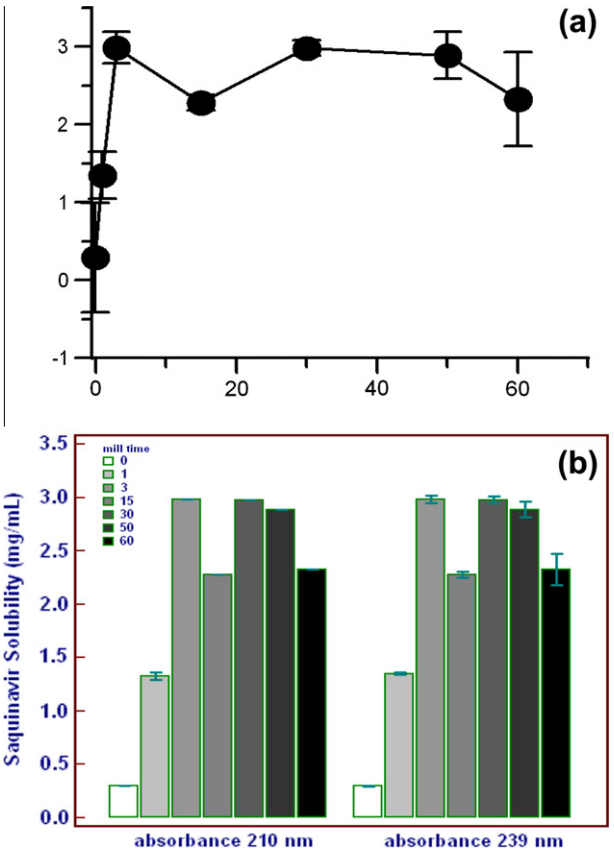

Fig. 11. Saquinavir solubility: (a) solubility verse milling time and (b) means clustered by groups' diagrams are shown. (For interpretation of the references to color in this figure legend, the reader is referred to the web version of this article.)

describe the effect of milling on drug powders. According to these studies, decreasing surface area increases the surface tension and each drug crystal has a specific dissolution pressure due to its particle size in the sub-micron range. The solubility enhancement therefore may hypothetically be predicted from the extent of size reduction in a drug solid [20,44]. Milling of a drug crystal also appears to induce partial lattice defects that propagate from the surface into the bulk of the solid [44,45]. These defects then promote partial transformation of the initial mass into the amorphous phase. This results in a solid–solid dispersion with lowered glass transition temperatures but higher aqueous solubility [44,45].

One study has suggested that the measurement or thermodynamic estimation of amorphous drug solubility is complicated by the inability to establish equilibrium of amorphous systems [46]. This metastable nature of amorphous solids after aggressive (more than 3 h) milling has been demonstrated in our studies as well. High-energy ball milling of SQVM results in drug products which occur as crystalline/amorphous mixtures that readily revert to more stable polymorphs or dispersions.

SQVM occurs as a highly crystalline drug powder with diffractograms distinguished by gradual lost of several crystalline peaks during the milling process. These diffractograms indicate an apparent polymorphic conversion, as observed by a return of some residual crystallinity at 60 h and a shift in high intensity salt peaks at 15 and 30 h. This conversion is further evidenced by changes in infrared spectra, BET surface area, pore structure, and solubility. One possible explanation for these observations suggests that formation of unstable amorphous structures appear after 15 h, which are characterized by greater pore size, but lower pore volume, surface area, and solubility. We suspect pore structure to extend into the bulk of the material rather than to be confined exclusively to the particle surface. However, the experimental distinction between surface and bulk porosity may only be determined by cross-sectional microscopy, thus the definitive pore structure is not yet certain.

5. Conclusions

Nanosizing and mechanical milling technologies offer unique opportunities for improvement of aqueous solubility and dissolution of antiretroviral drugs (ARVs). HIV protease inhibitors, although highly potent, are characterized by low oral bioavailability and limited penetration into the central nervous system. Our paper describes the preparation and assessment of ball milled saquinavir mesylate where its solubility in simulated saliva was increased (9-fold) by milling for 3 h. Increased milling (up to 60 h) time did not improve aqueous solubility but rather slightly decreased it due to the formation of metastable amorphous solids and or drug aggregates. The surface character of each of the milled powders indicates that nanoporous particles are formed which occur in crystalline/amorphous mixtures. These particles displayed different thermographic profiles typically with lowered glass transition and dehydration temperatures. The study also illustrates how long-range structure and physicochemical properties may potentially be controlled by milling time. Finally, no contamination of the drug by milling in stainless jars even after extended periods was observed. In conclusion, our findings present a suitable procedure for preparation of nanoporous anti-retroviral drugs with significantly improved solubility which might be useful in design of buccal drug delivery systems.

Acknowledgments

We are so much obliged to the National Research Foundation (NRF) and Medical Research Council (MRC) of Republic of South Africa, for providing the support to carry out the aforementioned work. We also thank Hoffman–La Roche Ltd., for donation of the drug product saquinavir mesylate, Priya Naidoo, UKZN School of Pharmacy, Neal Broomhead, UKZN School of Chemistry, and Dr. Gregory Malgas, CSIR Nanomaterials Characterization Facility for providing the helpful technical support.

References

[1] P. Sharma, S. Garg, Pure drug and polymer based nanotechnologies for the improved solubility, stability, bioavailability and targeting of anti-HIV drugs, Adv. Drug Deliv. Rev. 62 (2010) 491–502.
[2] G.C. Williams, P.J. Sinko, Oral absorption of the HIV protease inhibitors: a current update, Adv. Drug Deliv. Rev. 39 (1999) 211–238.
[3] Invirase (saquinavir mesylate) capsules, prescribing information. In: Physicians' Desk Reference, Medical Economics Data Production Co., Montvale, NJ, 1998, pp. 247–2475.
[4] H. Boudad, P. Legrand, G. Lebas, M. Cheron, D. Duchene, G. Ponchel, Combined hydroxypropyl-beta-cyclodextrin and poly(alkylcyanoacrylate) nanoparticles intended for oral administration of saquinavir, Int. J. Pharm. 218 (2001) 113–124.
[5] C.M. Buchanan, N.L. Buchanan, K.J. Edgar, J.L. Little, M.G. Ramsey, K.M. Ruble, V.J. Wacher, M.F. Wempe, Pharmacokinetics of saquinavir after intravenous and oral dosing of saquinavir: hydroxybutenyl-beta-cyclodextrin formulations, Biomacromolecules 9 (2008) 305–313.
[6] S.M. Pathak, P. Musmade, S. Dengle, A. Karthik, K. Bhat, N. Udupa, Enhanced oral absorption of saquinavir with methyl-beta-cyclodextrin—preparation and in vitro and in vivo evaluation, Eur. J. Pharm. Sci. 41 (2010) 440–451.
[7] M.E. Fitzsimmons, J.M. Collins, Selective biotransformation of the human immunodeficiency virus protease inhibitor saquinavir by human small-intestinal cytochrome P4503A4. Potential contribution to high first-pass metabolism, Drug Metab. Dispos. 25 (1997) 256–266.
[8] V.A. Eagling, D.J. Back, M.G. Barry, Differential inhibition of cytochrome P450 isoforms by the protease inhibitors, ritonavir, saquinavir and indinavir, Br. J. Clin. Pharmacol. 44 (1997) 190–194.
[9] J.C. Chaumeil, Micronisation: a method of improving the bioavailability of poorly soluble drugs, methods find, Exp. Clin. Pharmacol. 20 (3) (1998) 211–215.
[10] S. Agharkar, S. Lindenbaum, T. Higuchi, Enhancement of solubility of drug salts by hydrophilic counter-ions: properties of organic salts of an anti-malarial drug, J. Pharm. Sci. 65 (5) (1976) 747–749.
[11] K. Amin, R.-M. Dannenfelser, J. Zielinski, B. Wang, Lyophilization of polyethylene glycol mixtures, J. Pharm. Sci. 93 (9) (2004) 2244–2249.
[12] V.P. Torchillin, Micellar nanocarriers: pharmaceutical perspectives, Pharm. Res. 24 (2007) 1–16.
[13] R.A. Rajewski, V.J. Stella, Pharmaceutical applications of cyclodextrins. 2. In vivo drug delivery, J. Pharm. Sci. 85 (1996) 1142–1169.
[14] A.J. Humberstone, W.N. Charman, Lipid-based vehicles for the oral delivery of poorly soluble drugs, Adv. Drug Deliv. Rev. 25 (1997) 103–128.
[15] A.T. Florence, E.G. Salole, J.B. Stenlake, The effect of particle size reduction on digoxin crystal properties, J. Pharm. Pharmacol. 26 (1974) 479–480.
[16] K.C. Lee, J.A. Hersey, Crystal modification of methisazone by grinding, J. Pharm. Pharmacol. 29 (1979) 249–250.
[17] F. Muller, R.F. Polke, From the product and process requirements to the milling facility, Powder Technol. 105 (1999) 2–13.
[18] J. Hu, K.P. Johnston, R.O. Williams III, Nanoparticle engineering processes for enhancing the dissolution rates of poorly water soluble drugs, Drug Dev. Ind. Pharm. 30 (2004) 233–245.
[19] T. Takatsuka, T. Endo, J. Jianguo, K. Yuminoki, N. Hashimoto, Nanosizing of poorly water soluble compounds using rotation/revolution mixer, Chem. Pharm. Bull. 57 (2009) 1061–1067.
[20] J.A.H. Junghanns, R.H. Müller, Nanocrystal technology, drug delivery and clinical applications, Int. J. Nanomed. 3 (2008) 295–309.
[21] R.H. Muller, C. Jacobs, O. Kayser, Nanosuspensions as particulate drug formulations in therapy. Rationale for development and what we can expect for the future, Adv. Drug Deliv. Rev. 47 (1) (2001) 3–19.
[22] C.M. Keck, R.H. Muller, Drug nanocrystals of poorly soluble drugs produced by high pressure homogenization, Eur. J. Pharm. Biopharm. 62 (1) (2006) 3–16.
[23] E. Merisko-Liversidge, P. Sarpotdar, J. Bruno, S. Hajj, L. Wei, N. Peltier, J. Rake, J.M. Shaw, S. Pugh, L. Polin, J. Jones, T. Corbett, E. Cooper, G.G. Liversidge, Formulation and antitumor activity evaluation of nanocrystalline suspensions of poorly soluble anticancer drugs, Pharm. Res. 13 (1996) 272–278.
[24] T. Niwaa, Y. Nakanishib, K. Danjoa, One-step preparation of pharmaceutical nanocrystals using ultra cryo-milling technique in liquid nitrogen, Eur. J. Pharm. Sci. 41 (2010) 78–85.
[25] E. Merisko-Liversidge, G.G. Liversidge, E.R. Cooper, Nanosizing: a formulation approach for poorly water-soluble compounds, Eur. J. Pharm. Sci. 18 (2003) 113–120.
[26] C. Leuner, J. Dressman, Improving drug solubility for oral delivery using solid dispersions, Eur. J. Pharm. Biopharm. 50 (2000) 47–60.
[27] A.M. Kaushal, P. Gupta, A.K. Bansal, Amorphous drug delivery systems: molecular aspects, design, and performance, Crit. Rev. Ther. Drug Carrier Syst. 21 (2004) 133–193.
[28] M.G. Fakes, B.J. Vakkalagadda, F. Qian, S. Desikan, R.B. Gandhi, C. Lai, A. Hsieh, M.K. Franchini, H. Toale, J. Brown, Enhancement of oral bioavailability of an HIV-attachment inhibitor by nanosizing and amorphous formulation approaches, Int. J. Pharm. 370 (2009) 167–174.
[29] S. Sethia, E. Squillante, Solid dispersions: revival with greater possibilities and applications in oral drug delivery, Crit. Rev. Ther. Drug Carrier Syst. 20 (2003) 215–247.
[30] E.S. Kostewicz, M. Wunderlich, U. Brauns, R. Becker, T. Bock, J.B. Dressman, Predicting the precipitation of poorly soluble weak bases upon entry in the small intestine, J. Pharm. Pharmacol. 56 (2004) 43–51.
[31] A. Heinz, C.J. Strachan, F. Atassi, K.C. Gordon, T. Rades, Characterizing an amorphous system exhibiting trace crystallinity: a case study with saquinavir, Crystal Growth Des. 8 (2008) 119–127.
[32] S. Azarmi, W. Roa, R. Löbenberg, Current perspectives in dissolution testing of conventional and novel dosage forms, Int. J. Pharm. 328 (2007) 12–27.
[33] F.A. Mohamed, H. Khedr, Preparation and in vitro/in vivo evaluation of the buccal bioadhesive properties of slow-release tablets containing miconazole nitrate, Drug Dev. Ind. Pharm. 29 (2003) 321–337.
[34] S. Brunauer, P. Emmet, E. Teller, Adsorption of gases in multimolecular layers, J. Am. Chem. Soc. 60 (1938) 309–319.
[35] E. Barret, L.G. Joyner, P.P. Halenda, The determination of pore volume and area distributions in porous substances. I. Computations from nitrogen isotherms, J. Am. Chem. Soc. 73 (1951) 373–380.
[36] J.F. Bauer, W. Dziki, J.E. Quick, Role of an isomorphic desolvate in dissolution failures of an erythromycin tablet formulation, J. Pharm. Sci. 88 (1999) 1222–1227.
[37] G.A. Stephenson, E.G. Groleau, R.L. Kleeman, W. Xu, D.R. Rigsbee, Formation of isomorphic desolvates: creating a molecular vacuum, J. Pharm. Sci. 87 (1998) 536–542.
[38] H.G. Brittain, Effects of mechanical processing on phase composition, J. Pharm. Sci. 91 (2002) 1573–1580.
[39] P.G. Royall, D.Q.M. Craig, C. Doherty, Characterization of moisture uptake effects on the glass transitional behavior of an amorphous drug using modulated temperature DSC, Int. J. Pharm. 192 (1999) 39–46.
[40] F. Kesisoglou, S. Panmai, Y. Wu, Nanosizing – oral formulation development and biopharmaceutical evaluation, Adv. Drug Deliv. Rev. 59 (2007) 631–644.
[41] D.S. Singare, S. Marella, K. Gowthamarajan, G.T. Kulkarni, R. Vooturi, P.S. Rao, Optimization of formulation and process variable of nanosuspension: an industrial perspective, Int. J. Pharm. 402 (2010) 213–220.
[42] A.A. Date, V.B. Patravale, Current strategies for engineering drug nanoparticles, Curr. Opin. Colloid Interface Sci. 9 (2004) 222–235.
[43] Y. Kuo, H. Chen, Entrapment and release of saquinavir using novel cationic solid lipid nanoparticles, Int. J. Pharm. 365 (2009) 206–213.
[44] S. Desprez, M. Descamps, Transformation of glassy indomethacin by ball-milling, J. Non-Cryst. Solids 352 (2006) 4480–4485.
[45] G. Bruni, V. Berbenni, F. Sartor, C. Milanese, A. Girella, D. Franchi, A. Marini, Quantification methods of amorphous/crystalline fractions in high-energy ball milled pharmaceutical products, J. Therm. Anal. Calorim. 102 (2010) 297–303.
[46] B. Hancock, M. Parks, What is the solubility advantage for amorphous pharmaceuticals, Pharm. Res. 17 (2000) 397–404.
[47] E. Biazar, A. Beitollahi, S.M. Rezayat, T. Forati, A. Asefnejad, M. Rahimi, R. Zeinali, M. Ardesir, F. Hatamjafari, A. Sahebalzamani, M. Heidari, et al., Effect of the mechanical activation on size reduction of crystalline acetaminophen drug particles, Int. J. Nanomed. 4 (2009) 283–287.